Eur Biophys J (1985) 11:157–165

European Biophysics Journal

A molecular model for ion selectivity in membrane channels

H. Schröder

Fakultät für Physik, Universität Konstanz, Postfach 5560, D-7750 Konstanz, Federal Republic of Germany

Received July 24, 1984/Accepted September 24, 1984

Abstract. In this article, the three-dimensional motion of an ion within a molecular channel is discussed for the first time; escape rates from binding sites are calculated using the transition state method. For a given ligand configuration and a particular pore radius the rates depend upon ion size and mass. It is found that the activation energies depend strongly on the ion size, i.e., they increase with decreasing ion radius. In contrast to the rates obtained from the mass dependence alone, the rates depending on both mass and size of the alkali ions yield the completely inverted sequence, namely the Eisenman sequence I.

Key words: Ion-channel interaction, rate theory, ion transport, ion selectivity, Eisenman sequence

Introduction

Certain polypeptides, such as gramicidin A, when embedded in membranes, can form pores which support the passage of the alkali ions (Li^+, Na^+, K^+, Rb^+, and Cs^+) and similar particles. This transmembrane motion is possible only because molecular channels have the functional property of lowering the local energy barrier which is imposed on the ionic self energy by the presence of the membrane. In the case of gramicidin the central pore is lined with a helical arrangement of permanent, flexible dipoles, represented by carbonyl groups (Urry 1971; Urry et al. 1971). In the equilibrium orientation the oxygen atoms point toward the channel axis, negatively charging the interior of the pore. This effect is enhanced by orientational polarization in the presence of an ion, with its magnitude depending on the elasticity of the ligands (Schröder 1984). The response of the ligands should be the same for all monovalent ions, because of equal ionic charge, and the transport rates should vary with the law expected from rate theory, namely proportional to the inverse square root of the ion's mass. In fact, a wide range of ion specific selectivities for different channels is observed. For a given channel the effective transport rates of two different ionic species may vary by orders of magnitude. In general, even for the least preferred ions, the transport rates stay finite. Therefore different relative sequences of ion conductivity can be taken to be characteristic of different channels. Theoretically, the number of permutations possible for five ions should result in 120 observable sequences. However, the number of sequences actually observed in ion transport processes across membranes is only 11 and corresponds to the 11 Eisenman sequences first established and formulated for ion exchange selectivities of glass electrodes by Eisenman (1976).

Although this represents a relatively small range of possibilities, there is still no obvious reason why channels should behave so differently and why certain types of pores prefer heavier ions over lighter ones, while the conductivity sequence is inverted for other types. In the phenomenological view, a molecular channel is usually depicted as a sequence of barriers and binding sites (Partin and Eyring 1971; Woodbury 1971; Läuger 1973, 1979). The transport properties are represented by effective jump rates. In order to calculate the unidirectional current consisting of one ionic species across a sequence of n binding sites and $n+1$ barriers, a set of $2n+1$ independent parameters is necessary and can be found by fitting the effective rates to the observed current-voltage characteristics (Eisenman and Sandblom 1983). This procedure has to be repeated for each different ionic species. The resulting sets of effective rates are in general very different from each other and allow little or no insight into physical processes and causes. Actually, the effective rates incorporate very different phenomena, ranging from continuous diffusion in aqueous solution via dehydration to a discrete random walk within the pore. Since the sequence of barriers and binding sites reflects the potential profile as seen by a given ion along its diffusion path, the effective rates are really

not independent, but may derive from the interaction of the ion with its environment. Therefore it should be possible to describe the transport process for a certain channel and all alkali ions by a relatively small set of molecular parameters. That theoretical phenomenological rate descriptions for molecular channels and their environment are inappropriate to explain the true nature of transport and selectivity mechanisms can be seen by the fact that the smallest set of parameters possible is used to explain known experimental data, i.e., the number of effective rate constants does not necessarily correspond to the actual number of binding sites along the channel. In as much as the transmembrane motion of ions is a very complex process and performed in several, distinct steps, the motion through the channel interior must be mediated by several effects and countereffects, the exact composition of which gives rise to channel dependent (not environment dependent) selectivity rules.

In recently published articles (Schröder 1983a, b, 1984) the author has investigated the transport properties of a gramicidin-like channel model where the motion of the ion was restricted to the channel axis. It was shown that the ion and elastically bound ligands perform a coupled motion leading to an effective ion mass, which in turn depends on all ligand masses and the mutual interaction. It turned out that the appropriate picture of the migrating ion is that of a polaron (Schröder 1983b). Although the mass dependence of the corresponding jump rates may deviate considerably from the behavior predicted by the ART, especially for light ions, this modification can only partly explain the selectivity principles of a gramicidin-like channel, simply because a motion restricted to the channel axis is one-dimensional and cannot account for the ion's size. It is clear that an ion can only stay on the axis if its radius coincides with that of the pore. The smaller an ion is the more it can move off the axis. Consequently, a general three-dimensional diffusion path within the pore must be considered, and the relevant rate theory has to be formulated. This will be done in this article, for a channel with rigid ligands, in order to study the importance of size effects and to separate them from polarization effects. In the following section a general, model-independent derivation of the jump rates for three-dimensional motion inside the channel, – across saddle point and minima –, is given. In the last section a specific model is used to calculate the actual rates and to discuss the size effects for the alkali ions.

Ion-channel interaction in paraxial approximation and rate constants

Consider the Coulomb interaction $U(\vec{\mathbf{r}})$ of an ion within a pore, where the ligands and all other constituents parts of the molecular channel are arranged more or less cylindrically around a defined axis, for example, the z-direction. Then the ion is confined in the neighborhood of the axis and the potential may be expanded around $\vec{\varrho} = 0$, where $\vec{\varrho}$ is the position of the ion's centre of mass in the x-y-plane. Up to the second-order one obtains:

$$U(\vec{\mathbf{r}}) \simeq U(0,z) + \vec{\varrho}\,\frac{\partial U(\vec{\mathbf{r}})}{\partial \vec{\varrho}}\bigg|_{\vec{\varrho}=0} + \frac{1}{2}\left(\frac{\partial}{\partial \vec{\varrho}}\right)^2 U(\vec{\mathbf{r}})\bigg|_{\vec{\varrho}=0}. \tag{1}$$

Due to the low symmetry of the discrete distribution of ligands the coefficient

$$\frac{\partial U(\vec{\mathbf{r}})}{\partial \vec{\varrho}}\bigg|_{\vec{\varrho}=0}$$

will not be equal to zero. In contrast to the Coulomb interaction, the much more complex repulsive interaction occurs between the ion and all constituents parts of the channel. Thus it seems to be a fairly good approximation to assume an effective, "smeared out" potential of the form

$$\frac{1}{2}\varkappa_0 \varrho^2, \tag{2}$$

i.e., the first derivative with respect to $\vec{\varrho}$ vanishes by symmetry and $\varkappa_0$ is a constant.

This harmonic approximation of the non-Coulombic contribution to the total potential represents the interaction of the ion with the whole rest of the molecular channel and depends on ionic as well as on molecular properties. Combining (1) and (2) gives the total potential in the present approximation:

$$V(\vec{\mathbf{r}}) = U(0,z) + \vec{\varrho}\vec{\mathbf{A}}(z) + \frac{1}{2}\vec{\varrho}\,\vec{\mathbf{B}}(z)\vec{\varrho}$$

$$\vec{\mathbf{A}}(z) = \frac{\partial U(\vec{\mathbf{r}})}{\partial \vec{\varrho}}\bigg|_{\vec{\varrho}=0}$$

$$\vec{\mathbf{B}}(z) = 1 \cdot \varkappa_0 + \frac{\partial}{\partial \vec{\varrho}} \times \frac{\partial}{\partial \vec{\varrho}}\, U(\vec{\mathbf{r}})\bigg|_{\vec{\varrho}=0}. \tag{3}$$

For any position along the z-axis the equilibrium position $\vec{\varrho}_0(z)$ in the x-y-plane is given by:

$$\vec{\varrho}_0(z) = -\,\vec{\vec{\mathbf{B}}}^{-1}(z)\vec{\mathbf{A}}(z). \tag{4}$$

With $\vec{\vec{\mathbf{B}}} = \begin{pmatrix} B_{11} & B_{12} \\ B_{12} & B_{22} \end{pmatrix}$, stability in the position of the ion is guaranted by $B_{11} > 0$ and $B_{11}\,B_{22} - B_{12}^2 > 0$.

Under this condition, which can always be fulfilled by choosing a sufficiently large value of $\varkappa_0$, the

equilibrium path of the ion along the channel follows a sequence of saddle points. In the limit $\varkappa_0 \to \infty$ the deviation from the z-axis shrinks to zero, and the only surviving term of the potential is $U(0,z)$. Thus $\varkappa_0$ plays the role of a control parameter for the size of the ion, where increasing $\varkappa_0$ values can be directly related to increasing ionic radii. This relation will be established in the next section in connection with the chosen channel model. In order to arrive at the desired expression for the escape rate from a binding site it is very useful to start with the Lagrangian of the system:

$$L = \frac{1}{2} m \dot{\vec{r}}^2 - V(\vec{r}) . \tag{5}$$

Performing a change of variables by introducing the instantaneous deviation $\delta\vec{\varrho}$ from the equilibrium position $\vec{\varrho}_0$ of (4), we use

$$\vec{\varrho} = \vec{\varrho}_0 + \delta\vec{\varrho} \tag{6}$$

and can write:

$$L = \frac{1}{2} m \{\dot{z}^2 + (\dot{\vec{\varrho}}_0 + \delta\dot{\vec{\varrho}})^2\} - U(0,z)$$

$$+ \frac{1}{2} \vec{\mathbf{A}}\, \vec{\mathbf{B}}^{-1} \vec{\mathbf{A}} - \frac{1}{2} \delta\vec{\varrho}\, \vec{\mathbf{B}}\, \delta\vec{\varrho} . \tag{7}$$

Keeping in mind that $\vec{\varrho}_0$ is not an independent variable, i.e.

$$\dot{\vec{\varrho}}_0 = \frac{\partial\vec{\varrho}_0}{\partial z} \dot{z} ,$$

the longitudinal momentum of the ion is obtained as

$$\frac{\partial L}{\partial \dot{z}} = p_3 = m \left[1 + \left(\frac{\partial\vec{\varrho}_0}{\partial z}\right)^2\right] \dot{z} + m \frac{\partial\vec{\varrho}_0}{\partial z} \delta\dot{\vec{\varrho}} \tag{8}$$

and its transverse momentum as

$$\frac{\partial L}{\partial(\delta\dot{\vec{\varrho}})} = \vec{\mathbf{p}} = m \left(\delta\dot{\vec{\varrho}} + \frac{\partial\vec{\varrho}_0}{\partial z} \dot{z}\right) . \tag{9}$$

Equations (8) and (9) are readily solved for the velocities:

$$\dot{z} = \frac{1}{m} \left(p_3 - \vec{\mathbf{p}} \frac{\partial\vec{\varrho}_0}{\partial z}\right)$$

$$\delta\dot{\vec{\varrho}} = \frac{1}{m} \left[\vec{\mathbf{p}} + \frac{\partial\vec{\varrho}_0}{\partial z} \left(\frac{\partial\vec{\varrho}_0}{\partial z} \vec{\mathbf{p}}\right) - p_3 \frac{\partial\vec{\varrho}_0}{\partial z}\right] .$$

In the next step the usual Legendre transformation

$$H = \vec{\mathbf{p}}\, \delta\dot{\vec{\varrho}} + p_3 \dot{z} - L$$

yields the Hamiltonian

$$H = \frac{1}{2m} \vec{\mathbf{p}}^2 + \frac{1}{2m} \left(p_3 - \vec{\mathbf{p}} \frac{\partial\vec{\varrho}_0}{\partial z}\right)^2 - \frac{1}{2} \vec{\mathbf{A}} \vec{\mathbf{B}}^{-1} \vec{\mathbf{A}}$$

$$+ U(0,z) + \frac{1}{2} \delta\vec{\varrho}\, \vec{\mathbf{B}}\, \delta\vec{\varrho} , \tag{10}$$

which is expressed by the proper pairs of canonical variables. In case of the equilibrium situation, $\delta\vec{\varrho} = 0$, the effective potential is given by

$$V_{\text{eff}}(z) = V(z) - \frac{1}{2} \vec{\mathbf{A}}(z)\, \vec{\mathbf{B}}^{-1}(z)\, \vec{\mathbf{A}}(z) ,$$

$$V(z) = U(0,z) , \tag{11}$$

where the second term on the RHS is the correction due to the motion of the ion off the z-axis. It will be shown later that this term may contribute significantly to the interaction and vary strongly with the position along the axis, in contrast to $V(z)$.

The desired expression for the rate constants can easily be obtained by means of the transition state method (Pelzer and Wigner 1932; Eyring 1935). Following the procedure employed previously (Schröder 1983b), the ion-channel system represented by the Hamiltonian, (10), is subjected to temperature control. In thermal equilibrium, the state of the system is described by the Boltzmann distribution function, and the principle of detailed balance can be applied to calculate the escape rate across a given barrier as the average unidirectional current at the site of the corresponding saddle point.

Because of the symmetry of the system the current along the z-axis is the transport quantity of interest. The averaging process yields the following expression for the jump rate across the i-th barrier to the right:

$$k_i' = \frac{\int_0^\infty \mathrm{d}p_3\, \dot{z} \int \mathrm{d}^2\vec{\mathbf{p}} \int \mathrm{d}^2(\delta\vec{\varrho})\, e^{-\beta H}}{\int_{-\infty}^{\infty} \mathrm{d}p_3 \int \mathrm{d}^2\vec{\mathbf{p}} \int \mathrm{d}^3\vec{\mathbf{r}}\, e^{-\beta H}} , \quad \beta = \frac{1}{k_B T} . \tag{12}$$

With

$$V(\vec{\mathbf{r}}) = V(z) - \frac{1}{2} \vec{\mathbf{A}}\, \vec{\mathbf{B}}^{-1} \vec{\mathbf{A}} + \frac{1}{2} \delta\vec{\varrho}\, \vec{\mathbf{B}}\, \delta\vec{\varrho}$$

and

$$E_{\text{Kin}} = \frac{1}{2m} \vec{\mathbf{p}}^2 + \frac{1}{2m} \left(p_3 - \vec{\mathbf{p}} \frac{\partial\vec{\varrho}_0}{\partial z}\right)^2$$

the integrations in (12) may be written in detail as follows:

$$k_1' = \frac{\int_0^\infty \mathrm{d}p_3\ \dot{z}\ \int \mathrm{d}^2\,\vec{\mathbf{p}}\ \mathrm{e}^{-\beta E_{\mathrm{Kin}}}}{\int_{-\infty}^{\infty} \mathrm{d}p_3 \int \mathrm{d}^2\,\vec{\mathbf{p}}\ \mathrm{e}^{-\beta E_{\mathrm{Kin}}}} \cdot \frac{Q(z_i')}{\int_{z_{i-1}'}^{z_i'} \mathrm{d}z\ Q(z)}, \tag{13}$$

where z_{i-1}' and z_i' are the positions of adjacent saddle points. As a first step it is convenient to carry out the integration over p_3:

$$\int_0^\infty \mathrm{d}p_3\ \dot{z}\ \mathrm{e}^{-\frac{\beta}{2m}\left(p_3 - \vec{\mathbf{p}}\frac{\partial \vec{\varrho}_0}{\partial z}\right)^2}$$

$$= \frac{1}{m}\int_0^\infty \mathrm{d}p_3 \left(p_3 - \vec{\mathbf{p}}\frac{\partial \vec{\varrho}_0}{\partial z}\right) \mathrm{e}^{-\frac{\beta}{2m}\left(p_3 - \vec{\mathbf{p}}\frac{\partial \vec{\varrho}_0}{\partial z}\right)^2}$$

$$= \frac{1}{\beta}\,\mathrm{e}^{-\frac{\beta}{2m}\left(\vec{\mathbf{p}}\frac{\partial \vec{\varrho}_0}{\partial z}\right)^2}.$$

The remaining integration yields:

$$\int \mathrm{d}^2\vec{\mathbf{p}}\ \mathrm{e}^{-\frac{\beta}{2m}\left[\vec{\mathbf{p}}^2 + \left(\vec{\mathbf{p}}\frac{\partial \vec{\varrho}_0}{\partial z}\right)^2\right]} = \frac{2\pi m}{\beta\sqrt{1 + \left(\frac{\partial \vec{\varrho}_0}{\partial z}\right)^2}}.$$

After evaluating the integral in the denominator we obtain:

$$k_i' = \sqrt{\frac{kT}{2\pi m\left[1 + \left(\frac{\partial \vec{\varrho}_0}{\partial z}\right)^2\right]}} \cdot \frac{Q(z_i')}{\int_{z_{i-1}'}^{z_i'} \mathrm{d}z\ Q(z)}. \tag{14}$$

The integral involving the potential is the restricted sum of states:

$$Q(z) = \int \mathrm{d}^2(\delta\vec{\varrho})\ \mathrm{e}^{-\beta V(\vec{\mathbf{r}})}$$

$$= \mathrm{e}^{-\beta\left[V(z) - \frac{1}{2}\vec{\mathbf{A}}\,\vec{\mathbf{B}}^{-1}\vec{\mathbf{A}}\right]} \int \mathrm{e}^{-\frac{1}{2}\beta\,\delta\vec{\varrho}\,\vec{\mathbf{B}}\,\delta\vec{\varrho}}\,\mathrm{d}^2(\delta\vec{\varrho})$$

$$Q(z) = \frac{2\pi k_B T}{\sqrt{\det \vec{\mathbf{B}}}}\,\mathrm{e}^{-\beta\left[V(z) - \frac{1}{2}\vec{\mathbf{A}}\,\vec{\mathbf{B}}^{-1}\vec{\mathbf{A}}\right]}. \tag{15}$$

It can be expressed by the more familiar, temperature dependent potential, the so-called potential of the mean force. Let $Q(\infty)$ be the value of $Q(z)$ in the absence of the ion, then $V_{\mathrm{eff}}(z)$ is defined by the following relation,

$$Q(z) = Q(\infty)\,\mathrm{e}^{-\beta V_{\mathrm{eff}}(z)}.$$

where

$$Q(\infty) = \frac{2\pi k_B T}{\varkappa_0}: \tag{16}$$

Hence:

$$V_{\mathrm{eff}}(z) = V(z) - \frac{1}{2}\vec{\mathbf{A}}\,\vec{\mathbf{B}}^{-1}\vec{\mathbf{A}} - k_B T \ln\left(\frac{\varkappa_0}{\sqrt{\det \vec{\mathbf{B}}}}\right) \tag{17}$$

The difference between (11) and (17) is the entropy contribution

$$-\,k_B T \ln \frac{\varkappa_0}{\sqrt{\det \vec{\mathbf{B}}}},$$

which is finite for finite temperatures. Its presence in $V_{\mathrm{eff}}(z)$ reflects the fact that the equilibrium path of an ion as given by $\{z, \vec{\varrho}_0(z)\}$ is not the exact path but only the most probable one for finite temperatures.

It guarantees that the ion uses the most probable passage in the neighbourhood of a saddle point. With the use of the effective potential of (17) the rate is finally given as:

$$k_i' = \sqrt{\frac{k_B T}{2\pi m\left[1 + \left(\frac{\partial \vec{\varrho}_0}{\partial z}\right)^2\right]}} \cdot \frac{\mathrm{e}^{-\beta V(z_i')}}{\int_{z_{i-1}'}^{z_i'} \mathrm{d}z\ \mathrm{e}^{-\beta V_{\mathrm{eff}}(z)}}. \tag{18}$$

Due to the three-dimensional motion of an ion within a channel, there are three contributions in expression for the rate which distinguish it from the usual result of the ART in one dimension. Firstly, there are two corrections to the potential, one of which is entropic and both of which affect the activation energy and its dependence on the ion's size. Secondly, there is a purely geometrical contribution to the prefactor, which can be formulated as

$$\frac{\mathrm{d}s_0}{\mathrm{d}z} = \sqrt{1 + \left(\frac{\partial \vec{\varrho}_0}{\partial z}\right)^2}, \tag{19}$$

where $\mathrm{d}s_0$ is the line element of the equilibrium path. It tells us that the rate decreases with increasing length of the average reaction path. Effectively the prefactor is the projection of the thermal velocity along the path into the z-axis, where the derivative has to be taken at $z = z_i'$.

If desired, $V_{\mathrm{eff}}(z)$ can be replaced by its harmonic expansion around the minimum and inserted into (18). This procedure yields the low temperature limit of the rate in the form of the Arrhenius law.

Numerical model calculations

The present model is identical with the channel model used for earlier investigations except for the fact that the ligands are assumed to be rigid. It may be considered as a crude approximation to the gramicidin A

channel, at least with respect to the Coulomb interaction. The carbonyl groups are simulated by permanent dipoles in a helical array (Fischer and Brickmann 1983). The dipoles possess a constant moment $p = q'\mathrm{d}$ with an effective charge $q' = 0.4\,\mathrm{e}$ and length $\mathrm{d} = 1.24$ Å. One helical turn includes six dipoles with alternating orientations on a constant radius with $\varrho_0 = 3$ Å. The pitch is 6 Å, thus the lattice constant along the z-axis is 1 Å. The whole channel consists of five turns with a total length of 30 Å. Since the purpose of the present investigation is to study ion size dominated selective effects for a given configuration, we neglect the head-to-head binding effect of the dimer (Pullmann and Etchebest 1983). The potential $U(\vec{\mathbf{r}})$ is given by the sum of all ion-dipole pair interactions:

$$U(\vec{\mathbf{r}}) = -q \sum_{\mu=1}^{30} \frac{\vec{\mathbf{p}}_\mu(\vec{\mathbf{r}} - \vec{\mathbf{r}})}{|\vec{\mathbf{r}} - \vec{\mathbf{r}}_\mu|^3}$$

$$= -q \sum_{\mu=1}^{30} \frac{p_{z\mu}(z - z_0\mu) + \vec{\mathbf{p}}_{\perp\mu}(\vec{\varrho} - \vec{\varrho}_\mu)}{\sqrt{(z - z_0\mu)^2 + (\vec{\varrho} - \vec{\varrho}_\mu)^2}^3}. \quad (20)$$

Here z_0 is the lattice constant and $\varrho_0 = |\vec{\varrho}_\mu|$. Each dipole is parallel to a plane with the z-axis. Thus $\vec{\mathbf{p}}_{\perp\mu}$ is parallel to $\vec{\varrho}_\mu$ for each μ, where

$$p_{z\mu} = p \cdot \cos\vartheta_\mu$$

and

$$|\vec{\mathbf{p}}_{\perp\mu}| = p \cdot \sin\vartheta_\mu .$$

It is convenient to use the relation

$$\vec{\mathbf{p}}_{\perp\mu} = \lambda\vec{\varrho}_\mu$$

with

$$\lambda = \frac{p}{\varrho_0}\sin\vartheta_\mu .$$

Hence the resulting expression for the potential is

$$U(\vec{\mathbf{r}}) =$$

$$-q\,p \sum_{\mu=1}^{30} \frac{(z - z_0\mu)\cos\vartheta_\mu + \varrho_0(\vec{\varrho}\vec{\varrho}_\mu/\varrho_0^2 - 1)\sin\vartheta_\mu}{\sqrt{(z - z_0)^2 + (\vec{\varrho} - \vec{\varrho}_\mu)^2}^3}, \quad (21)$$

which is to be expanded around $\vec{\varrho} = 0$. For $\vec{\varrho} = 0$ we obtain from (21) the zeroth-order term

$$V(\zeta) = -V_0 \sum_{\mu=1}^{30} \frac{(\zeta - \mu)\cos\vartheta_\mu - \Delta \cdot \sin\vartheta_\mu}{\sqrt{(\zeta - \mu)^2 + \Delta^2}^3} \quad (22)$$

where we have used

$$V_0 = \frac{p\,q}{z_0^2}, \quad \zeta = \frac{z}{z_0}, \quad \text{and} \quad \Delta = \frac{\varrho_0}{z_0}.$$

In the same notation the first derivative with respect to $\vec{\varrho}$ yields:

$$\vec{\mathbf{A}}(\zeta) = -\frac{V_0}{z_0}\sum_\mu \hat{\varrho}_\mu \left\{\frac{\sin\vartheta_\mu}{\sqrt{(\zeta - \mu)^2 + \Delta^2}^3}\right.$$

$$\left. + 3\,\Delta \cdot \frac{(\zeta - \mu)\cos\vartheta_\mu - \Delta \cdot \sin\vartheta_\mu}{\sqrt{(\zeta - \mu)^2 + \Delta^2}^5}\right\}, \quad (23)$$

where $\hat{\varrho}_\mu$ is the vector of unity in the molecular x-y-plane

$$\hat{\varrho}_\mu = \begin{pmatrix}\cos\phi_\mu \\ \sin\phi_\mu\end{pmatrix},$$

pointing towards the positions of the dipoles, and

$$\phi_\mu = \frac{\pi}{3}\mu .$$

The second derivative of the potential, (3), yields the tensor $\ddot{\mathbf{B}}(\zeta)$:

$$\ddot{\mathbf{B}}(\zeta) = 1 \cdot \varkappa_0 + 3\frac{V_0}{z_0^2}\sum_\mu \left\{\frac{(\zeta - \mu)\cos\vartheta_\mu - \Delta \cdot \sin\vartheta_\mu}{\sqrt{(\zeta - \mu)^2 + \Delta^2}^5}\right.$$

$$- \hat{\varrho}_\mu \times \hat{\varrho}_\mu \left[2\,\frac{\Delta \cdot \sin\vartheta_\mu}{\sqrt{(\zeta - \mu)^2 + \Delta^2}^5}\right.$$

$$\left.\left. + 5\,\Delta\,\frac{(\zeta - \mu)\cos\vartheta_\mu - \Delta \cdot \sin\vartheta_\mu}{\sqrt{(\zeta - \mu)^2 + \Delta^2}^7}\right]\right\}. \quad (24)$$

Introducing the dimensionless quantities $\hat{A}_i$ and $\hat{B}_{ij}$ with the relations:

$$\vec{\mathbf{A}}(\zeta) = -\frac{V_0}{z_0}\begin{pmatrix}\hat{A}_1 \\ \hat{A}_2\end{pmatrix}$$

and

$$\ddot{\mathbf{B}}(\zeta) = 3\frac{V_0}{z_0^2}\begin{pmatrix}\hat{B}_{11}\,\hat{B}_{12} \\ \hat{B}_{12}\,\hat{B}_{22}\end{pmatrix}$$

the effective potential according to (17) is:

$$V_{\text{eff}}(\zeta) = -V_0 \sum_{\mu=1}^{30} \frac{(\zeta-\mu)\cos\vartheta_\mu - \Delta \cdot \sin\vartheta_\mu}{\sqrt{(\zeta-\mu)^2+\Delta^2}^3}$$

$$-\frac{1}{6} V_0 \frac{\hat{B}_{22}\hat{A}_1^2 - 2\hat{B}_{12}\hat{A}_1\hat{A}_2 + \hat{B}_{11}\hat{A}_2^2}{\hat{B}_{11}\hat{B}_{22} - \hat{B}_{12}^2}$$

$$-k_B T \ln\left\{\frac{\varkappa}{\sqrt{\hat{B}_{11}\hat{B}_{22} - \hat{B}_{12}^2}}\right\}. \qquad (25)$$

Here we use a further dimensionless quantity

$$\varkappa = \frac{\varkappa_0 z_0^2}{3 V_0}$$

instead of $\varkappa_0$. Accordingly, the equilibrium position of the ion in the x-y-plane is given by:

$$\vec{\varrho}_0(\zeta) = \frac{1}{3}\frac{z_0}{\hat{B}_{11}\hat{B}_{22} - \hat{B}_{12}^2}\begin{pmatrix} \hat{B}_{22}\hat{A}_1 - \hat{B}_{12}\hat{A}_2 \\ -\hat{B}_{12}\hat{A}_1 + \hat{B}_{11}\hat{A}_2 \end{pmatrix}. \qquad (26)$$

All summations in the coefficients given above run over all ligand positions and have to be performed numerically. This procedure requires the input of the position dependent orientations ϑ_μ, which are free parameters in this model. In order to obtain a gramicidin-like structure, orientationally alternating dipoles in the following sequence are used:

$$\vartheta_\mu = \vartheta_0$$

$$\vartheta_{\mu+1} = 180° - \vartheta_0\,,$$

where $\vartheta_0 = -20°$ and $\vartheta_1 = \vartheta_0$.

For these and the other parameters values given before the effective potential, (25), has been alculated for several $\varkappa$ values and a constant temperature, $T = 300°$ K. The results are shown in Figs. 1 and 2. In both cases the potential is given in units of temperature. Figure 1 shows the potential profile from outside the channel to the centre for two $\varkappa$ values. Both curves display a sharp drop in potential as soon as the ion enters the channel. This effect is due to the orientation of the dipoles towards the molecular axis, which results in an excess of negative charge in the interior. For $\varkappa = \infty$ the motion of the ion is confined to the z-axis, whereas it can move about rather freely for $\varkappa = 0.03$. In the first case the resolution is not very high (the activation energy is only some 30° K at most), because the distance between the ion and the nearest dipole is always large compared to the separation of neighbouring dipoles. In the second case considered the situation is very different. Here the ion can come very close to each individual dipole, and well defined binding sites are the consequence. The activation energy reaches a remarkable 2,000° K. Thus, what a channel looks like, depends very much on the mobility of the ion. The effect of varying $\varkappa$ is shown in Fig. 2. Here the profile of the central binding site is shown for various values of $\varkappa$. Since the activation energies change drastically with $\varkappa$, an even greater dependence of the rates on this parameter is to be expected, including strong selectivity effects.

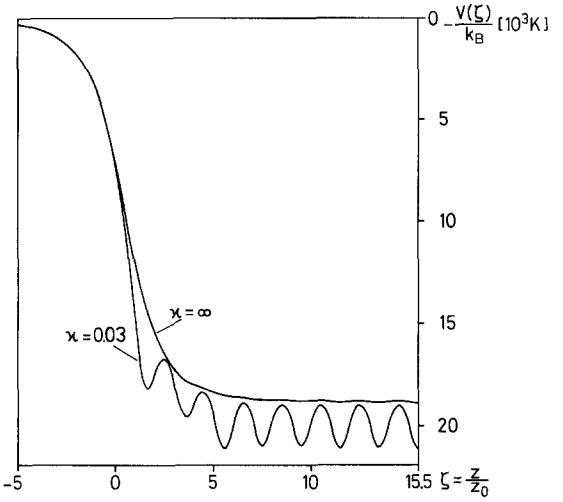

Fig. 1. The channel profile shown for motion restricted to the z-axis, ($\varkappa = \infty$), and three-dimensional motion, ($\varkappa = 0.03$)

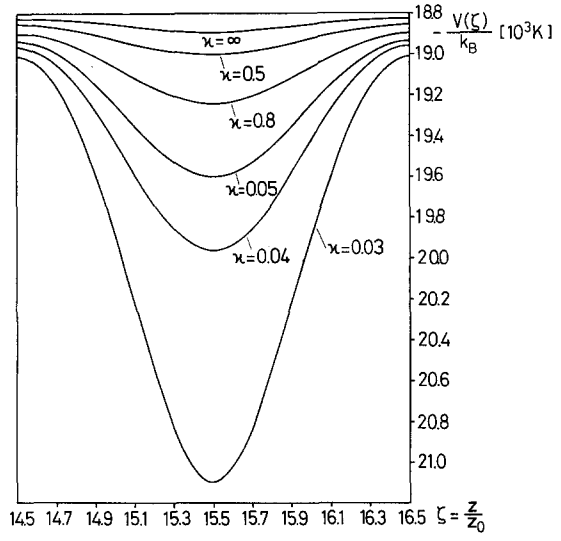

Fig. 2. The profile of the central binding site shown for several values of the control parameter, $\varkappa$, for the ion's size

Up to this point the missing link has been relation between ion mass and size on one side and $\varkappa$ on the other. It is clear that at this level an ab initio calcula-

tion is neither desirable nor possible. However, if the known data for ion radius and mass are used as input parameters, one either needs a relation between mass and $\varkappa$ or radius and $\varkappa$. As it turns out, the choice of the latter is consistent with the model developed here and is easy to establish. Consider an average radius, R, of the pore and ion radius, R_I. Then the deviation of the ion's center from the channel axis cannot be larger than pore radius minus ion radius, i.e., this difference defines $|\vec{\varrho}_{\mathrm{Max}}|$:

$$|\vec{\varrho}_{\mathrm{Max}}| = R - R_I\,.$$

On the other hand $|\vec{\varrho}_{\mathrm{Max}}|$ is a function of $\varkappa$. In Fig. 3 the equilibrium path of an ion for $\varkappa = 0.0326$ has been plotted according to (26). Inside the channel the path can be considered to be periodic with a 3-fold symmetry about the z-axis, neglecting end effects. The ion reaches its largest distance from the z-axis periodically, with the same value of $|\vec{\varrho}_0| = |\vec{\varrho}_{\mathrm{Max}}|$, in a position between the negative ends of a pair of dipoles. In order to identify a given ionic radius with the relevant value of $\varkappa$, one has to look for that $\varkappa$, which satisfies (27) for a given R. This procedure is illustrated in Fig. 4. Here $|\vec{\varrho}_{\mathrm{Max}}|$ has been plotted as a function of $\varkappa$. The average radius of the pore, R, has been chosen as 2 Å, which corresponds to the radius of the central hole in a gramicidin channel. For the ions their Pauling radii have been used. The result is the following list of parameters:

Li^+ :	$R_I = 0.60$ Å	$\lvert\vec{\varrho}_{\mathrm{Max}}\rvert = 1.40$ Å	$\varkappa = 0.0296$
Na^+ :	$R_I = 0.95$ Å	$\lvert\vec{\varrho}_{\mathrm{Max}}\rvert = 1.05$ Å	$\varkappa = 0.0326$
K^+ :	$R_I = 1.33$ Å	$\lvert\vec{\varrho}_{\mathrm{Max}}\rvert = 0.67$ Å	$\varkappa = 0.0395$
Rb^+ :	$R_I = 1.48$ Å	$\lvert\vec{\varrho}_{\mathrm{Max}}\rvert = 0.52$ Å	$\varkappa = 0.0449$
Cs^+ :	$R_I = 1.69$ Å	$\lvert\vec{\varrho}_{\mathrm{Max}}\rvert = 0.31$ Å	$\varkappa = 0.0615$

In the last step rates have been calculated for the central binding site (Fig. 2) for $T = 300°$ K, according to (18). For each of the five ion masses the rate has been plotted as a function of $\varkappa$ (Fig. 5). At any given point on the $\varkappa$-axis the rates follow the $m^{-1/2}$ law, i.e., the Eisenman sequence XI is obtained. Along each constant-mass-curve there is only one point which corresponds to the relevant ionic radius. It has been fixed by the relevant value of $\varkappa$, previously identified and marked by a cross in Fig. 5. The numbers obtained for the rates are:

Li^+ : $k' = 2.789 \cdot 10^9\ s^{-1}$
Na^+ : $k' = 9.147 \cdot 10^9\ s^{-1}$
K^+ : $k' = 4.559 \cdot 10^{10}\ s^{-1}$
Rb^+ : $k' = 6.022 \cdot 10^{10}\ s^{-1}$
Cs^+ : $k' = 1.138 \cdot 10^{11}\ s^{-1}$

This is clearly the Eisenman sequence I with respect to a single binding site. Thus the size effect

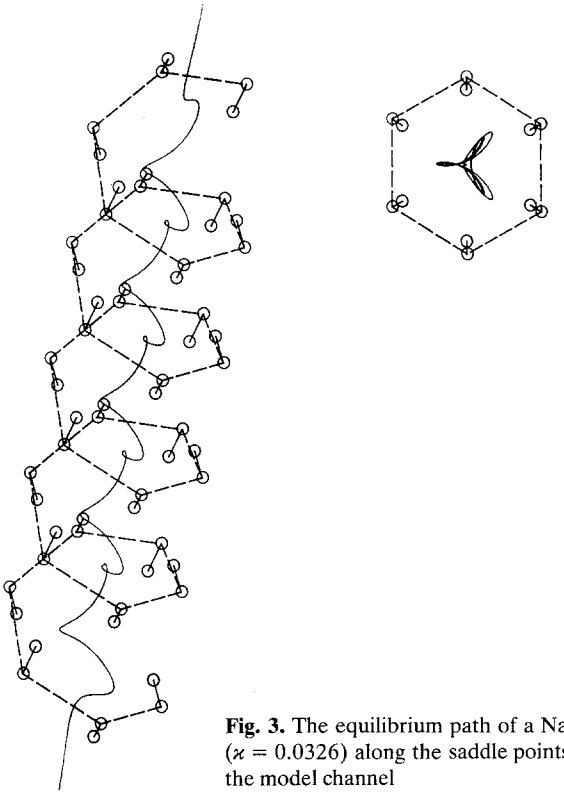

Fig. 3. The equilibrium path of a Na^+-ion ($\varkappa = 0.0326$) along the saddle points of the model channel

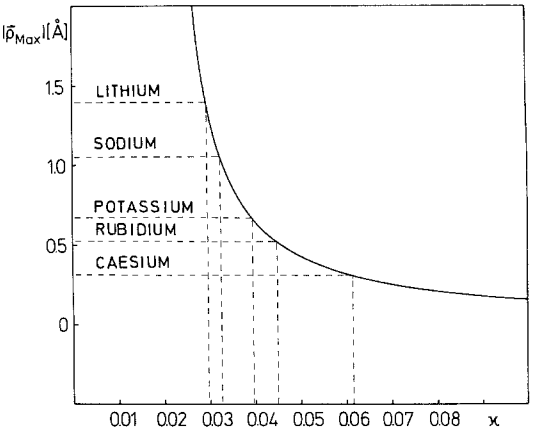

Fig. 4. The periodic maximum deviation $|\vec{\varrho}_{\mathrm{Max}}|$ off the channel axis plotted as a function of $\varkappa$. The identification of $\varkappa$ with the relevant ionic radius (dashed lines) has been made for a pore radius of 2 Å

sufficiently dominates over mass effect to invert the sequence determined by the ion masses alone. A similar result can be obtained for any of the other 15 binding sites, apart from the fact that for any site other than the central one the rates to the left and the right, respectively, are not equal.

The Eisenman sequence I corresponds to the mobility of the respective ions in water, a result that is due to hydrodynamic forces. On the other hand, this is also the observed sequence for the gramicidin A

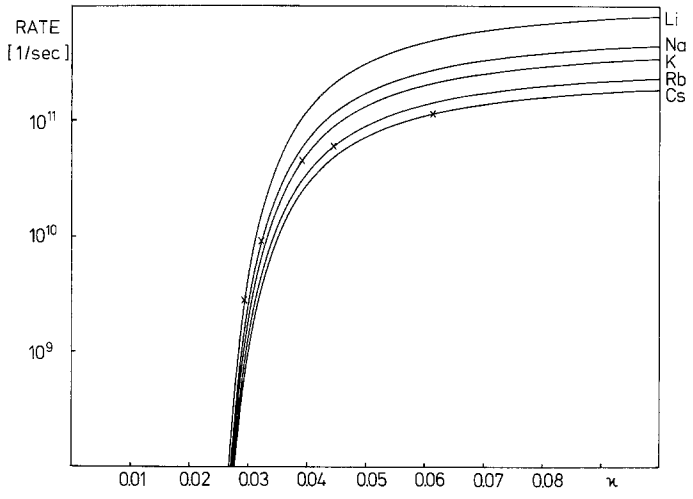

Fig. 5. The jump rates of the alkali ions are plotted as functions of $\varkappa$. Along each curve the ion mass is kept constant

channel. Moreover, the same sequence has been found for the present model which resembles basic features of the interactions in a gramicidin channel. However, conclusions from such analogies should be drawn with the greatest care. For instance, the actually observed transport quantities for gramacidin have to be taken as effective rates, i.e., they are referring to the channel in its natural environment, and not only to the channel interior as in the present model and therefore must be seen as the result of complex processes. Whereas the primary task is the explanation of an observed selectivity sequence by means of a molecular model, it is certainly a fascinating question in itself as to whether this coincidence in three different cases is accidental or possibly due to some very simple, basic mechanism. This decision requires a more refined model, which takes into consideration the coupled motion of ion and ligands and their restoring forces. From previous considerations the polaron character of the system is known. Similar behavior is to be expected for a system with the ion in three-dimensional motion; this will be the subject of a forthcoming paper. Since a polarizable channel is more realistic than the present model, it leads to a better understanding of possible selectivity principles.

For another important reason the polarizability of a channel is of great interest. Ions in aqueous solution carry a hydration shell. Upon entering the interior of a channel-like molecule, some of the water molecules have to be stripped off the ion for steric and energetic reason. For this process it seems to be very important that the channel can respond to the presence of the ion. If the interior is lined with flexible ligands the polarization effect of the ion with respect to the former is the same as with respect to accompanying water molecules. In such pores the reorienting ligands may replace some of the water molecules of the former hydration shell and thus significantly lower the effective dehydration energy. On the other hand an appropriate equilibrium orientation and additional polarization of the ligands lowers the energy barrier imposed on the self-energy of the penetrating ion by the presence of the membrane (Schröder 1984).

Discussion

The subject of this investigation has been the introduction of a parameter controlling the ion's size in the expression for the jump rates. The approach chosen, the paraxial approximation, can be considered as model independent as long as the definition of an equilibrium path, i.e., a space curve along saddle points in a pore like formation of ligands or lattice points, is possible. General results for the equilibrium path and the rate constants have been derived, and numerical calculations habe been performed for a model resembling the gramicidin channel. The size parameter is determined by an effective pore radius, the respective ion radius and the resulting maximum possible distance of the ion's center from the channel axis. For finite temperatures fluctuations of the position around the three-dimensional equilibrium path can occur, leading to an entropic contribution in the effective potential. However, the non-entropic correction to the potential due to the deviation from the channel axis is strongly size dependent and dominating, whereas the contribution due to the motion along the axis is size independent. The expression for the rate, i.e., the average lifetime of an ion in a binding site, features a competition between ion mass and size. It turns out that the activation energy decreases with increasing mass. This competition effect leads to an inversion of the originally mass determined selectivity sequence. Whereas the increase in the activation energy with decreasing ion size leads directly to a longer mean residence time, an effectively longer path for smaller ions also contributes, in the form of a geometrical prefactor, to even lower rates. The results is the Eisenman sequence I.

Acknowledgement. This work has been supported financially by the DFG (Heisenberg-Programm).

References

Eisenman G (1967) Glass electrodes for hydrogen and other cations: principles and practic. Marcel Dekker, New York

Eisenman G, Sandblom JP (1983) Energy barriers in ionic channels: Data for gramicidin A interpreted using a single file (3B4S'') model having 3 barriers separating 4 sites. In: Spach G (ed) Physical chemistry of transmembrane ion motions. Proceedings of 36th International Conference of Société de Chimie Physique. Elsevier, Paris, p 329

Eyring H (1935) The activated complex in chemical reactions. J Chem Phys 3: 107

Fischer W, Brickmann J (1983) Ion-specific diffusion rates through transmembrane protein channels. A molecular dynamics study. Biophys Chem 18: 323

Läuger P (1973) Ion transport through pores: A rate-theory analysis. Biochim Biophys Acta 311: 423

Läuger P (1979) Ion transport across Lipid bilayer membranes. In: Stevens CF, Tsien RW (eds) Membrane transport processes. Raven, New York, vol 3

Partin B, Eyring H (1971) In: Clarke MT (ed) Ion transport across membranes. Academic Press, New York, pp 103–118

Pelzer H, Wigner E (1932) Über die Geschwindigkeitskonstante von Austauschreaktionen. Z Phys Chem B 15: 445

Pullman A, Etchebest C (1983) The gramicidin A channel: The energy profile for single and double occupancy in a head-to-head $\beta^{6,3}_{3,3}$-helical dimer backbone. FEBS Lett 163: 199

Schröder H (1983a) Transit time conception for ion diffusion through membrane channels. J Chem Phys 79: 1991

Schröder H (1983b) Rate theoretical analysis of ion transport in membrane channels with elastically bound ligands. J Chem Phys 79: 1997

Schröder H (1984) Model calculation of polarization effects in elastic membrane channels. Biophys Chem. 20: 157–173

Urry DW (1971) The gramicidin A transmembrane channel: A proposed $\pi_{(L,D)}$ helix. Proc Natl Acad Sci USA 68: 672

Urry DW, Goodhall MC, Gliekson JD, Mayers DF (1971) The gramicidin A transmembrane channel: Characteristics of head-to-head dimerized $\pi_{(L,D)}$ helices. Proc Natl Acad Sci USA 68: 1907

Woodbury JW (1971) Eyring rate theory model of the current-voltage relationship of ion channels in excitable membranes. In: Hirschfelder F (ed) Chemical dynamics. Papers in honor of Henry Eyring. Wiley, New York